Design and measurements of a broadband two-dimensional acoustic metamaterial with anisotropic effective mass density

Lucian Zigoneanu,[1] Bogdan-Ioan Popa,[1] Anthony F. Starr,[2] and Steven A. Cummer[1,a]

[1]*Department of Electrical and Computer Engineering, Duke University, Durham, North Carolina 27708, USA*
[2]*SensorMetrix, Incorporated, 10211 Pacific Mesa Blvd., Suite 408, San Diego, California 92121, USA*

We present the experimental realization and characterization of a broadband acoustic metamaterial with strongly anisotropic effective mass density. The metamaterial is composed of arrays of solid inclusions in an air background, and the anisotropy is controlled by the rotational asymmetry of these inclusions. Transmission and reflection measurements inside a one-dimensional waveguide are used to extract the relevant components of the effective density tensor together with the effective bulk modulus of the metamaterial. Its broadband anisotropy is demonstrated by measurements that span 500–3000 Hz. Excellent agreement between these measurements and numerical simulations confirms the accuracy of the design approach. © *2011 American Institute of Physics*. [doi:10.1063/1.3552990]

I. INTRODUCTION

Acoustic metamaterials have gained extensive attention in the last several years due to their ability to exhibit material properties that are challenging to obtain in natural materials. Intensive research has been conducted in order to determine the basic physics behind these materials and their possible applications. For example, various engineered materials with negative effective density and/or negative bulk modulus have been demonstrated.[1–4] Applications for these kinds of materials have been demonstrated and include the acoustic superlens[5] and the magnifying acoustic hyperlens[6] that can exceed the diffraction limit in imaging and are easier to manufacture than conventional lenses along with acoustic absorbing panels[7] with higher transmission loss and smaller thicknesses than regular absorbers. Most of these approaches rely on resonant inclusions and the resulting acoustic metamaterial parameters vary strongly with frequency.

The quest for acoustic metamaterials has been partly inspired by the success obtained for their counterparts, electromagnetic (EM) metamaterials. For the EM case, Maxwell's equations are invariant to coordinate transformation. This leads to the concept of transformation electromagnetics[8] in which arbitrary bending and stretching of EM waves is possible with the proper electromagnetic material parameters. Although the elastodynamic wave equations are not transformation invariant in general,[9] it was first shown that for the two-dimensional (2D) case the acoustic wave equations are transformation invariant.[10] It was later shown that the three-dimensional (3D) acoustic wave equations are transformation invariant[11,12] if the way in which the velocity vector and pressure scalar change is different than the way in which electric and magnetic field vectors change in the EM case.[12] This work has led to the concept of transformation acoustics, in which the arbitrary bending of acoustic waves can be realized using acoustic metamaterials that generally have anisotropic mass density. Several material design methods have been proposed in order to achieve this anisotropy and to control the effective material parameters in the desired way: elastic cylinders with a special spatial arrangement,[13] concentric multilayers of isotropic sonic crystals,[14,15] rigid inclusions disposed in an array,[16,17] arrays of fluid cavities joined by piezoelectric edges,[18] or Helmholtz resonators with piezoelectric diaphragms.[19]

Here, we expand upon previous work[17] and demonstrate experimentally that relatively simple solid inclusions in a fluid or gas background can create an anisotropic effective mass density. From the simulations point of view, it has been shown that one unit cell is sufficient in order to compute the effective material parameters of this type of unit cell.[17] Thus, we use this procedure to design a broadband 2D acoustic metamaterial with anisotropic mass density and measure its effective properties from acoustic reflection and transmission measurements, using two orientations to obtain two components of the mass density tensor. A mass anisotropy ratio of 2.4 is obtained, in excellent agreement with the simulations, and the samples exhibit broadband effective mass and bulk modulus that vary minimally from 1000 to 3000 Hz. These measurements demonstrate that the approach used in Ref. 17 can be utilized to design relatively simple broadband and anisotropic acoustic metamaterial structures suitable for many transformation acoustics applications.

II. UNIT CELL DESIGN AND SIMULATION

Our aims constrain the metamaterial design presented here in the following ways. First, we need the effective material properties to be broadband, i.e., they should remain relatively unchanged in a large frequency range. Second, in order for our engineered material to be described in terms of effective material parameters, the unit cell used to generate the structure has to be significantly subwavelength. Third, the material must exhibit effective mass anisotropy with the ratio between the relevant components of the mass density

---
a)Author to whom correspondence should be addressed. Electronic mail: cummer@ee.duke.edu.
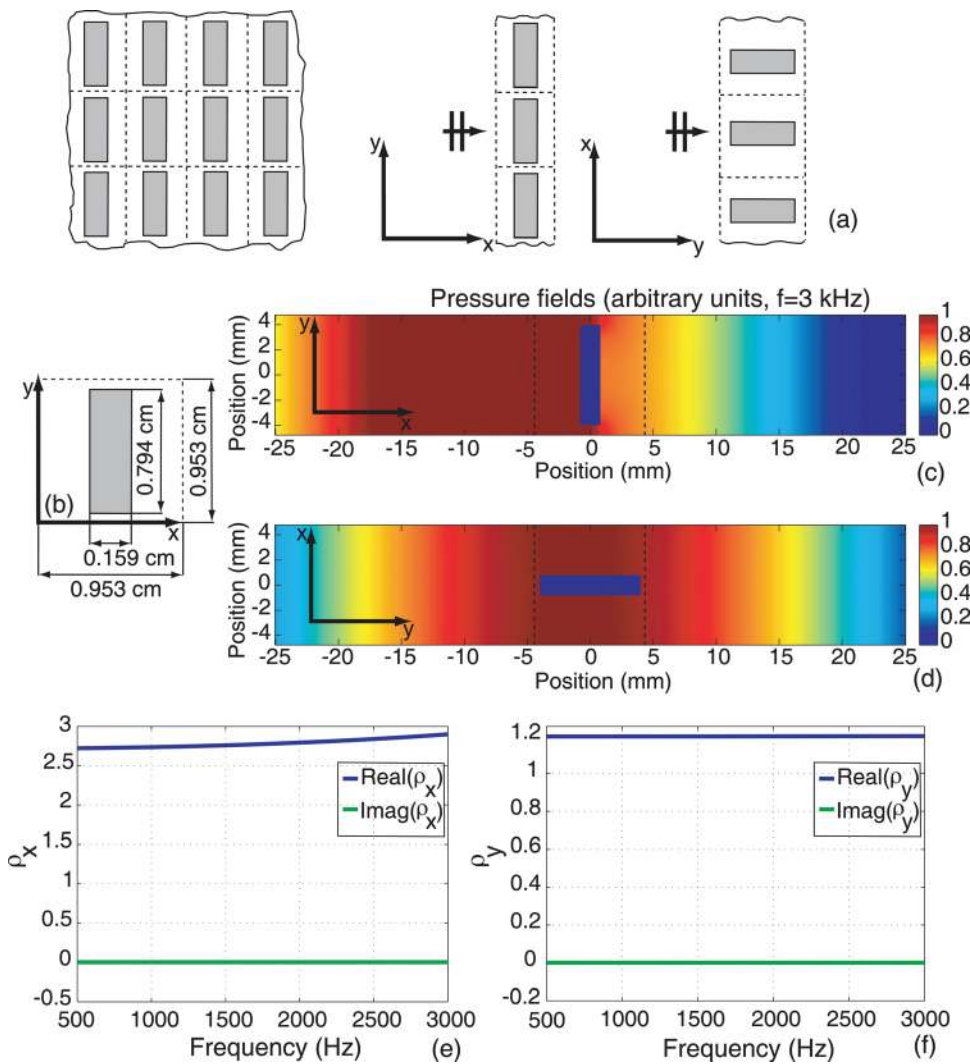
109, 054906-1

FIG. 1. (Color online) (a) Left: metamaterial composed of arrays of identical unit cells. Middle: one cell thick metamaterial sample used to obtain one component of the effective density tensor ρ_x. Right: one cell thick metamaterial sample used to obtain the second component of the effective density tensor ρ_y. (b) Unit cell used to analyze the effective material properties and its orientation; (c) simulations for acoustic plane wave propagation in the x direction ($f = 3$ kHz); (d) simulations for acoustic plane wave propagation in the y direction ($f = 3$ kHz); (e) broadband effective mass density in the x direction; (f) broadband effective mass density in the y direction.

tensors of at least 2. We choose a somewhat arbitrary value of 2.4, which is typical for materials needed to realize designs based on transformation acoustics.

Our engineered material is made of arrays of identical unit cells, as illustrated on the left side of Fig. 1(a). Using the procedure described in Ref. 17 we designed a unit cell satisfying the above constraints. Its structure is presented in Fig. 1(b). The background fluid is air and is characterized by a bulk modulus of $\lambda_0 = 141$ kPa and a density of $\rho_0 = 1.29$ kg/m^3. The cell dimension is 9.53 mm $\times$ 9.53 mm and consists of a rectangular block of aluminum ($\lambda_{Al} = 68.9$ GPa, $\rho_{Al} = 2712.63$ kg/m^3) of dimensions 1.59 mm $\times$ 7.94 mm placed in the middle of the cell. It is the rotational asymmetry in the geometry of this aluminum inclusion that is responsible for the anisotropic behavior of the cell. We align the coordinate system so that the x and y axes are perpendicular and respectively, parallel to the longest side of the rectangular inclusion.

As described in Ref. 17 the effective material parameters associated with the metamaterial are retrieved from two numerical simulations performed with COMSOL Multiphysics in which plane waves are sent through the metamaterial from two different angles. We are using the Acoustic-Structure Interaction module (frequency response analysis) and all

the elastic properties of the solid inclusions are taken into consideration. More specifically, in order to obtain the effective bulk modulus and the component of the effective density tensor in the x direction, we send a plane wave along the x axis through a thin metamaterial sample. It has been shown[17] that a sample as thin as one unit cell in the propagation direction and infinitely long in the transverse direction can be used in order to obtain accurate effective parameters. Such a sample is shown in the middle section of Fig. 1(a). The other relevant component of the density tensor can be obtained by sending a plane wave along the y direction through a similar thin slab of metamaterial, as illustrated on the right side of Fig. 1(a).

The slab infinite extent in the transverse direction is simulated in COMSOL Multiphysics through the use of rigid walls. This allows efficient one cell simulations that result in the effective parameters of the bulk metamaterial. The pressure fields computed for each direction of incidence are presented in Figs. 1(c) and 1(d). These fields are used to determine the complex reflection and transmission coefficients in each case. The coefficients are then inverted using the procedure described in Ref. 20 in order to obtain the effective material parameters. Given the dimensions specified above, the two relevant components of the effective
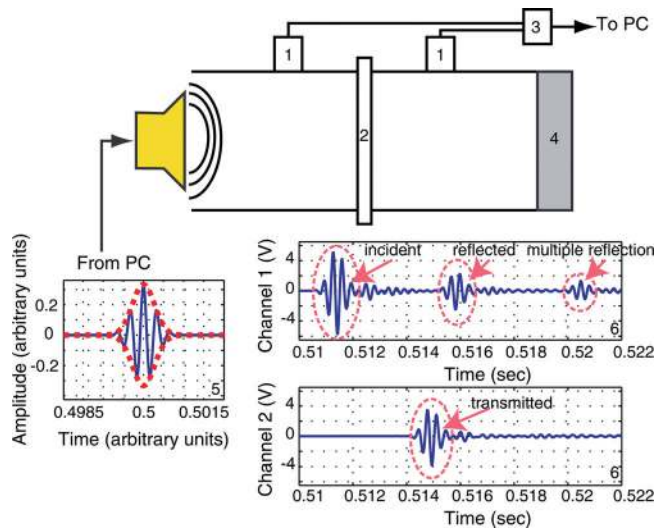
FIG. 2. (Color online) Experimental setup: 1—microphone and preamplifier; 2—sample holder; 3—NI terminal block; 4—anechoic termination; 5—example of the signal sent from a PC; 6—example of signals collected at the microphones before the sample (top) and after the sample (bottom).

mass density tensor associated with the unit cell (relative to the air density) are, at the design frequency of 3 kHz, $\rho_x = 2.9$ and $\rho_y = 1.2$. As shown in Figs. 1(e) and 1(f), one component of effective mass density is essentially invariant with frequency across the entire 500–3000 Hz band, while the larger component varies minimally from 2.7–2.9 across the same frequency band. The orientation of the x and y axes relative to the unit cell is specified in Fig. 1(b). We note that the unit cell is at least 1 order of magnitude smaller than the background wavelength at 3 kHz, which allow us to effectively apply the homogenization theory in this case. The anisotropy factor at 3 kHz, $\rho_x/\rho_y = 2.41$ exceeds our requirement of being at least 2.

III. MEASUREMENT DETAILS

The primary goal of this work is to experimentally validate the effective parameters of the unit cell designed theoretically in the previous section. We characterize fabricated metamaterial samples using the same procedure employed above in the simulations: we send plane waves through metamaterial samples and measure and invert the obtained complex transmission and reflection coefficients in order to retrieve the effective material parameters.

The experimental setup used to generate the acoustic plane wave-material interaction and to measure the reflection and transmission coefficients is presented in Fig. 2. The waveguides are circular pipes of ABS plastic of 7.62 cm inner diameter and 0.635 cm in thickness. The waveguide cutoff frequency is 2.63 kHz, below which only the useful fundamental mode propagates. Above this frequency, a second mode starts to propagate, however its group velocity is considerably lower than the velocity of the fundamental mode. Therefore, the time domain processing technique allows us to separate the pulses corresponding to the two

modes for frequencies up to around 4 kHz, and consequently allows us to accurately characterize materials inside the waveguide at frequencies in our target range of DC to 3 kHz.

The sound source is an external speaker 7.62 cm in diameter and the anechoic termination placed at the end of the second tube is made of polystyrene foam. The microphones are unidirectional electret condenser microphones and were chosen based on their relatively small size, 6 mm in diameter, and good sensitivity from 100 Hz–12 kHz. The microphone locations are fixed in positions to ensure that the incident and reflected signals are distinct. The signals from each microphone preamplifier are digitally sampled at 44.1 kHz with 16 bit resolution, and the transmitted speaker waveforms are digitally generated.

The input signal transmitted from the speaker through the acoustic waveguide is presented in Fig. 2, and consists of a Gaussian pulse modulated with a sinusoidal signal at the desired frequency, f_0:

$$s_i(t) = \exp[-0.74(f_0 t)^2]\cos(2\pi f_0 t). \tag{1}$$

The width of the Gaussian pulse was chosen based on two criteria. First, the bandwidth of the input signal has to be small enough that the sample under test has effective material parameters constant in that bandwidth. Second, the duration of the pulse must be small enough so that the incident portion of the measured signal and the multiple reflections caused by the sample under test and the termination of the waveguide are sufficiently separated in time to allow easy retrieval of phase and amplitude (see Fig. 2 for typical measured waveforms). Since the samples under test are broadband, we chose a Gaussian pulse width of approximately five periods of the sinusoidal signal of frequency f_0. We explore the frequency range from 500 Hz–3 kHz and perform measurements and simulations every 100 Hz. The central frequency of the Gaussian pulse is the same as the frequency analyzed (e.g., for 500 Hz, $f_0 = 500$ Hz). The ratio of full width half power bandwidth to central frequency in this case is 0.455. This is a relatively wide bandwidth that would be unsuitable to characterize materials that exhibit strong frequency dispersion. However, the effective parameters of this material are nearly constant with frequency (see Fig. 6), and the wide pulse bandwidth does not affect the reliability of the measurements.

In order to increase the signal-to-noise ratio, 10 independent sequential measurements are averaged. The complex reflection and transmission coefficients are computed using the signals collected from both channels and two reference signals: the signal measured with no sample (perfect transmission) and the signal measured with a solid, thick Al disk (perfect reflection). These reference signals are used to calibrate the attenuation and speed variations of the propagating wave due to phenomena such as changes in temperature inside the waveguide.

The reflection coefficient amplitude and phase are computed as follows.

First, we align the three signals recorded by the first microphone with the sample under test, no sample, and a solid disk with respect to one of them [Fig. 3(a)]. This
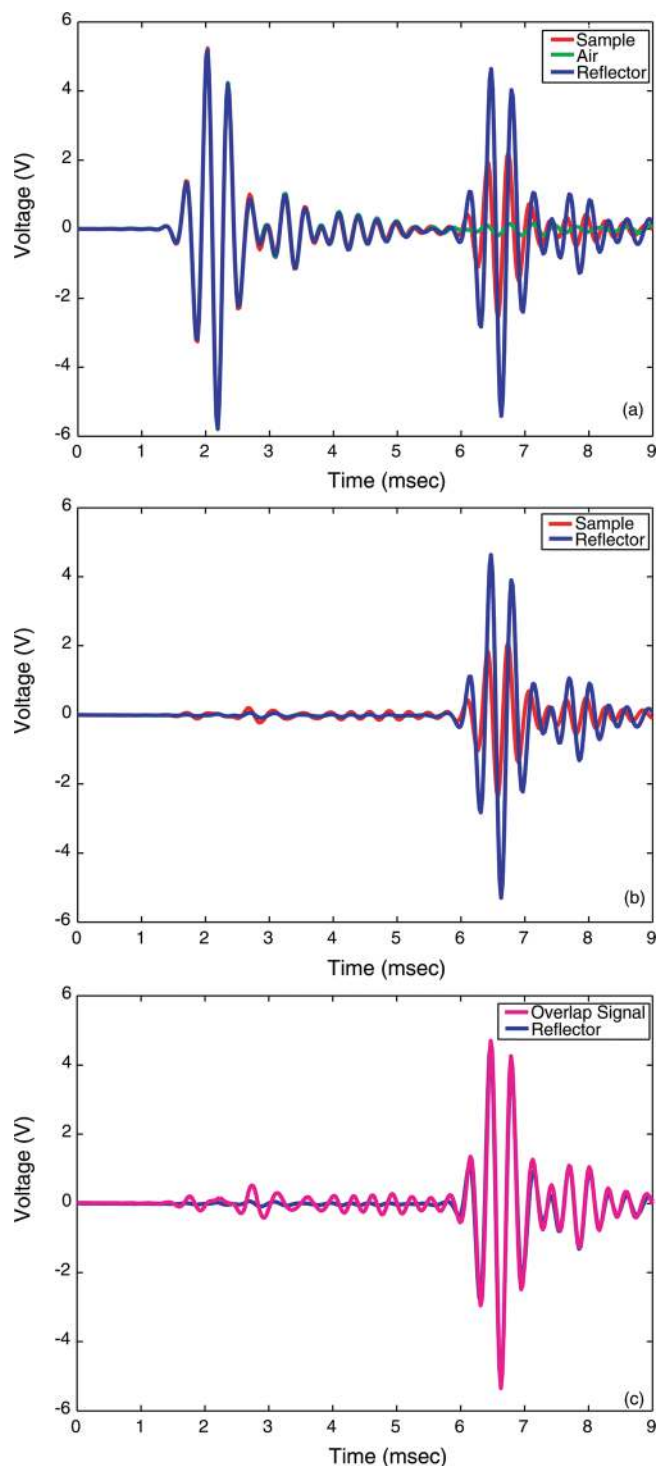
FIG. 3. (Color online) Example of signals used to determine the reflection and transmission coefficients: (a) initial signals collected at Channel 1 with sample, air, and perfect reflector (incident signal and first reflection, aligned); (b) isolated first reflection; and (c) reflected signal from the sample modified in amplitude and phase to overlap over the signal from the perfect reflector.

alignment is necessary because of the differences in time processing of the PC (i.e., the incident signal measured at the first channel should be at the same moment in time for all measurements). Then, we use the same time shift to move the signals recorded by the second microphone (i.e., the signals should be recorded at the same time for the two

channels). Second, we isolate the signal reflected by the sample under test (s_1), e.g., the line labeled "Sample" in Fig. 3(b) (subtract the signal measured with no sample from the signal measured with the sample under test). We compare this signal to the similar signal produced by the perfect reflector (s_2) (e.g., the line labeled "Reflector" in Fig. 3(b)), and determine the delay, phase, and amplitude change needed by s_1 in order to for it to overlap s_2 using the translation and scaling properties of their Fourier transform (e.g., the line labeled "Overlap Signal" in Fig. 3(c)). These phase and amplitude corrections represent, from definition, the phase and amplitude of the reflection coefficient. A similar procedure is used for computing the transmission coefficient. This time we compare the incident portion of the signals transmitted to the second channel when there is a sample in the tube and when there is no sample in the tube (perfect transmission). We find that this time domain retrieval method proves reliable and robust for relatively broadband samples.

IV. EXPERIMENTAL MEASUREMENTS

In order to experimentally measure the effective parameters of our anisotropic engineered material, we fabricated the two material samples shown in the middle and on the right side of Fig. 1(a). As discussed previously, both samples are one unit cell thick in the propagation direction and fill
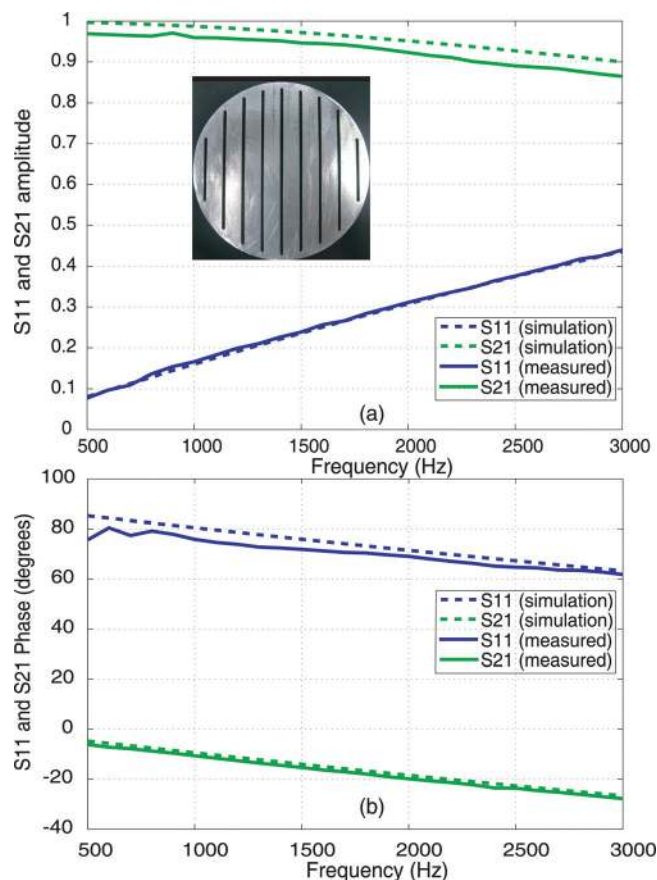

FIG. 4. (Color online) Propagation in the *x* direction. Reflection and transmission coefficients (a) amplitude and (b) phase.
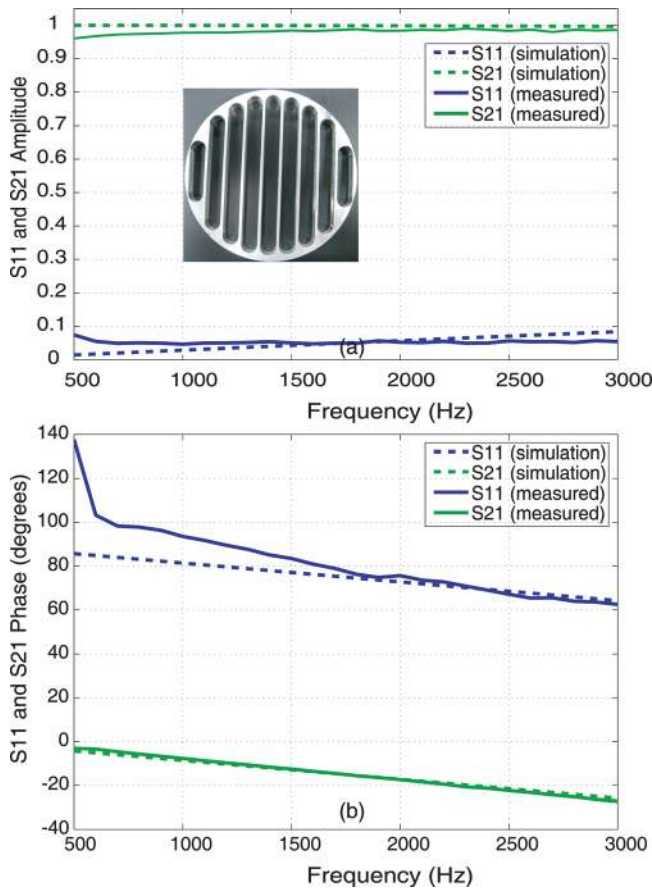
FIG. 5. (Color online) Propagation in the *y* direction. Reflection and transmission coefficients (a) amplitude and (b) phase.

the entire transverse section of the waveguide in order to simulate an infinite extent in the plane perpendicular to the direction of propagation. The samples were made with Al

because it is highly available and easy to machine. Figure 4 shows the measured reflection and transmission coefficients [amplitude (a) and phase (b)] in the *x* direction (which corresponds to the upper configuration in Fig. 1), compared with the expected results produced by simulations. Generally excellent agreement between the simulations and the measured reflection and transmission coefficients, both amplitude and phase, is observed. The transmission coefficient is approximately 3% lower than the expected value across the entire frequency range. We attribute this small discrepancy to pressure leakage around the sample in the system and the accuracy of our measurements could perhaps be improved by using a different mechanism for holding the sample and the microphones or by better sealing the joints between the samples and tubes.

Similarly, a separate set of measurements was performed for the pressure plane wave propagating in the *y* direction (Fig. 5), which corresponds to the lower configuration in Fig. 1. Excellent agreement between simulations and measurements is observed for the amplitude and phase of both coefficients. Again, the measured transmission coefficient is a few percent smaller than the predicted values from numerical simulations across the entire frequency range.

We note that the measured phase of the reflection coefficient starts to diverge from the simulation at low frequencies below 1.5 kHz. This behavior is mainly caused by two factors. First, the sample is acoustically thin at low frequencies, therefore, the reflected signal is very weak and the low signal-to-noise ratio does not allow reliable processing of the phase information. Although the inclusion size could be considered small compared with the wavelength at low frequencies for propagation in the *x* direction also, this dimension is five times larger. Therefore, the reflected signal is about five times larger (e.g., 0.09 compared with 0.02 at 500 Hz), which translates into a higher signal-to-noise ratio. This
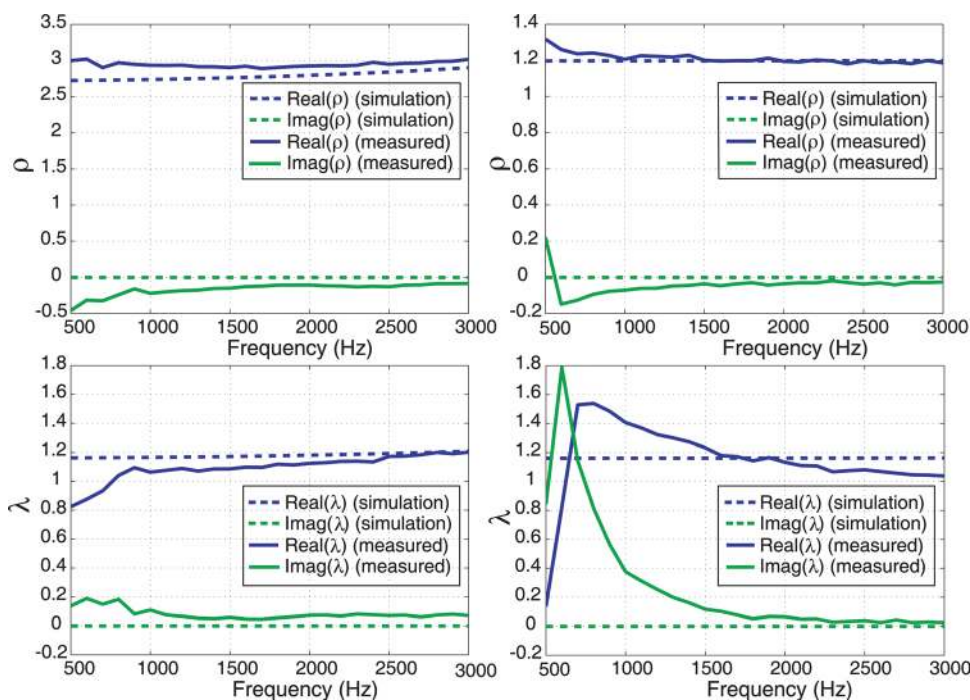

Figure 6. (Color online) Effective mass density and bulk modulus in the *x* (left column) and *y* (right column) directions.

explains the larger discrepancy between the measured and simulated phase of the reflection coefficient when the incident wave propagates in the y direction compared to the case in which the wave propagates along the x direction. Second, at these lower frequencies the pulse due to the first reflection (needed during the retrieval) partly overlaps with the incident pulse and subsequent reflections, which, once again decreases the effectiveness of the phase retrieval at these low frequencies.

Using the transmission and reflection coefficients, we computed the effective mass density and bulk modulus in both directions, x and y, using the procedure described in Sec. II.[20] These measured effective parameters are shown in Fig. 6.

For both directions, the measured effective material parameters closely match the expected results over the entire 500 Hz–3 kHz bandwidth. The measured effective mass densities are nearly invariant with frequency and are in excellent agreement with simulations in both orientations. The measured mass anisotropy ratio varies from 2.28 to 2.54 from 500–3000 Hz, which is in extremely close agreement with the simulated value. The relative mass density exceeds one in both directions as expected because the Al inclusions have a density greater than the surrounding background.

The effective bulk modulus is about 1.2 (relative to the air bulk modulus) in both directions of propagation and it is measured to be nearly independent of frequency over much (but not all) of the frequency band. For propagation in the y direction, the challenges in accurately measuring small reflection magnitudes leads to significant measurement discrepancies in the bulk modulus below 1.5 kHz. This can be seen from the expression of the bulk modulus written as a function of the reflection and transmission coefficients[20]

$$\lambda = \sqrt{\frac{(1 + S_{11})^2 - S_{21}^2}{(1 - S_{11})^2 - S_{21}^2}} k_0 d \left[\arccos \frac{1 - S_{11}^2 + S_{21}^2}{2S_{21}} \right]^{-1}, \quad (2)$$

where k_0 is the wavenumber in air, and d is the sample thickness. From this equation we notice that

$$\lim_{S_{11} \to 0; \, S_{21} \to 1} \frac{\partial \lambda}{\partial S_{11}} = \infty, \quad (3)$$

which means that the bulk modulus becomes very sensitive to small variations of the measured reflection coefficient S_{11} at low frequencies where the acoustic thickness of the sample becomes very small.

V. CONCLUSIONS

We have demonstrated that the effective material parameters of anisotropic acoustic metamaterials designed with the approach presented in Ref. 17 can be verified experimentally using 1D waveguide measurements. The technique was demonstrated by designing a broadband metamaterial with significant effective mass anisotropy made of solid inclusions placed in a background fluid (air, in our case). The complex reflection and transmission coefficients of two samples that correspond to two orthogonal orientations of the same unit cell were measured over a 500–3000 Hz bandwidth, and then inverted to obtain the effective mass density tensor components and the bulk modulus.

The measurements confirm that the metamaterial design exhibits strong effective mass anisotropy and nearly frequency-independent effective properties. In one direction, the measured effective relative (to air) mass density was within a few percent of the simulated value of 1.2 across the full bandwidth, while in the orthogonal direction the measured density was within less than 10% of the simulated value, again across the full bandwidth. Modest (several tenths of a percent) disagreement was observed in the measured bulk modulus below 1 kHz for one orientation, but this is entirely attributable to the sensitivity of this parameter to the measured reflection coefficient, which was small (< 0.1) for this orientation.

This work validates a technique to design and characterize strongly anisotropic and broadband acoustic metamaterials, and is thus a valuable tool in the design of broadband devices obtained through the technique of transformation acoustics.

[1] Z. Yang, J. Mei, M. Yang, N. H. Chan, and P. Sheng, Phys. Rev. Lett. **101**, 204301 (2008).
[2] J. Li and C. T. Chan, Phys. Rev. **E 70**, 055602(R) (2004).
[3] S. H. Lee, C. M. Park, Y. M. Seo, Z. G. Wang, and C. K. Kim, Phys. Lett. A **373**, 4464 (2009).
[4] N. Fang, D. J. Xi, J. Y. Xu, M. Ambati, W. Srituravanich, C. Sun, and X. Zhang, Nature Mater. **5**, 452 (2006).
[5] S. Zhang, L. L. Yin, and N. Fang, Phys. Rev. Lett. **102**, 194301 (2009).
[6] J. S. Li, L. Fok, X. B. Yin, G. Bartal, and X. Zhang, Nature Mater. **8**, 931 (2009).
[7] Z. Yang, H. M. Dai, N. H. Chan, G. C. Ma, and P. Sheng, Appl. Phys. Lett. **96**, 041906 (2010).
[8] J. B. Pendry, D. Schurig, and D. R. Smith, Science **312**, 1780 (2006).
[9] G. W. Milton, M. Briane, and J. R. Willis, New J. Phys. **8**, 248 (2006).
[10] S. A. Cummer and D. Schurig, New J. Phys. **9**, 45 (2007).
[11] H. Y. Chen and C. T. Chan, Appl. Phys. Lett. **91**, 183518 (2007).
[12] S. A. Cummer, M. Rahm, and D. Schurig, New J. Phys. **10**, 112025 (2008).
[13] D. Torrent and J. Sanchez-Dehesa, New J. Phys. **10**, 023004 (2008).
[14] D. Torrent and J. Sanchez-Dehesa, New J. Phys. **10**, 063015 (2008).
[15] Y. Cheng, F. Yang, J. Y. Xu, and X. J. Liu, Appl. Phys. Lett. **92**, 151913 (2008).
[16] J. B. Pendry and J. Li, New J. Phys. **10**, 115032 (2008).
[17] B. I. Popa and S. A. Cummer, Phys. Rev. B **80**, 174303 (2009).
[18] A. Baz, New J. Phys. **11**, 123010 (2009).
[19] W. Akl and A. Baz, J. Intell. Mater.Syst. Struct. **21**, 541 (2010).
[20] V. Fokin, M. Ambati, C. Sun, and X. Zhang, Phys. Rev. B **76**, 144302 (2007).